A SIMULATION STUDY ON HYDROTHERMAL SYSTEM OF THE KAKKONDA GEOTHERMAL FIELD

Norio Arihara*, Hiroshi Yoshida*, Mineyuki Hanano**, and Ken Ikeuchi**

*
** Waseda University, 3-4-1 Ohkubo, Shinjuku-ku, Tokyo 169, Japan
JMC Geothermal Engineering Co., Ltd., Ukai, Takizawa-mura, Iwate 020-01, Japan

Key words: simulation, fracture, injection, aquifer, hydrothermal mechanism

ABSTRACT

The hydrothermal system of the Kakkonda geothermal field, an active liquid-dominated reservoir, has been studied by a three-dimensional dual porosity geothermal model. Development of the field started first by exploiting a reservoir which ranges from 1000 to 1500 m in depth. After about eight years of production and injection in this reservoir, another reservoir was found below the first one. A unique feature has been confirmed such that the hydrothermal connection of the two reservoirs is very weak, and that the lower reservoir shows much higher temperature than the upper reservoir.

Hydrothermal mechanisms confirmed by simulation are the existence of an extensive thermal aquifer which sustains the pressure of the upper reservoir, and a very limited communication between the reservoirs.

1. INTRODUCTION

Development of the Kakkonda geothermal field, located in the northern part of the main land, Japan, can be divided into two phases. The first phase was initiated in 1978 when a 50 MWe power plant was started with 11 producers and 15 injectors. The reservoir developed in this phase is liquid-dominated and ranges from 1000 to 1500 m in depth. Some 50 production, injection and testing wells have additionally been drilled. The injectors were initially completed in the producing area but shallower than the producing zones. After about 12 years of operation, aditional injectors were drilled into the producing zones, but about 1.5 km away from the production area.

During the first phase, several clues were observed to suggest the existence of another reservoir below the first. Kasai et al. (1990) described that some wells drilled down to 1500 m showed temperatures jumping from about 250°C to over 300°C, and hot water inflow at this temperature level. Tosha et al. (1993) presented a micro-earthquake hypocenter distribution in a cross-section which clearly shows fracture development through Pre-Tertiary formation.

The deeper reservoir was confirmed by an exploration well drilled in 1986 and also by the first deep production well drilled in 1989. The latter is fully described by Saito (1993). The field development has then entered into the second phase in which the develoment of the deeper reservoir is planned in order to sustain the first power plant and also to install the second power plant of 30 MWe. Seven production wells to supply 325 tons/hr steam have been successfully completed for these purposes, as reported by Sato (1992).

Geology of the field has been reported in detail by several authors (Sato, 1982, Doi et al., 1988, Kato and Doi, 1993, Kato et al., 1993). As seen in a conceptual model shown in Fig. 1, the major geologic sequence from top is Tertiary formation, Pre-Tertiary formation and neo-granite pluton. Tertiary formation is locally divided into 3 formations, i.e. 1) Y formation which includes siltstone, mudstone and sandstone, 2) T formation which is mainly dacitic tuff, and 3) K formation. K formation is composed of three sub-formations: Upper-K and Middle-K formations which are mainly dacitic tuff with much shale, and Lower-K formation which is mainly andesitic tuff. Pre-Tertiary formation includes acidic tuff, sandstone and slate as well as tonalite intruding into formation.

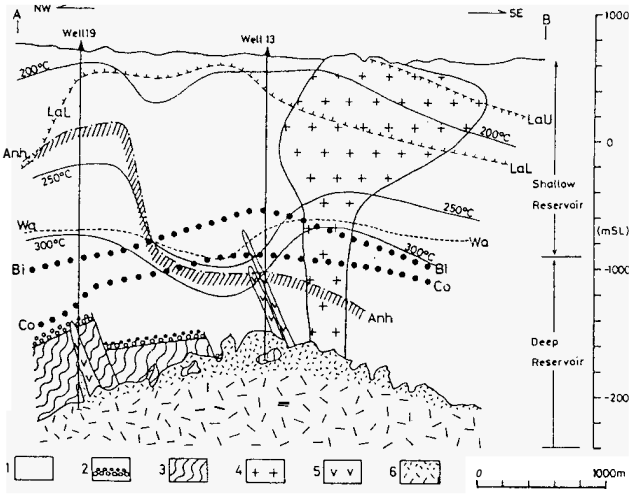

1 Tertiary formation, 2 Basal conglomerate in Tertiary formation, 3 Pre-Tertiary formation, 4 Dacitic intrusion. 5 Old tonalite intrusion. 6. Neo-tonalite or quartz diorite pluton. LaU Upper limit of laumontite, LaL Lower limit of laumontite, Anh: Upper limit of anhydrite, Wa. Lower limit of wairakite, Bi: Biotite isograd, Co: Cordierite isograd

Fig. 1 - Schematic geologic cross-section at the Kakkonda geothermal field (after Kato et al., 1993).

Neo-granitic pluton composed of tonalite and quart diorite appears at 2200 - 2800 m in depth. This neo-granitic pluton caused thermal metamorphosing of rocks in Middle-K, Lower-K and Pre-Tertiary formations. Main metamorphic minerals are biotite and cordierite. Their isograds are also shown in Fig. 1. Relative depths of these isograds can be correlated with top depths of neo-granitic pluton.

The boundary between the upper and lower reservoirs is located at the top of Lower-K formation. The interval 1000 - 1600 in in Upper- and Middle-K formations is highly fractured and forms the main producing zone of the upper reservoir. Lower-K and Pre-Tertiary formations are generally tight. The fractured productive zone of the lower reservoir exists at the top of the neo-granitic pluton.

The principal objectives of this study are to construct an appropriate model of the reservoir, and to analyze the hydrothennal mechanism by simulation

2. SIMULATION MODEL

Structural geometries and property distributions for the model were first prepared based on various data and the interpreted results such as the conceptual model, structural maps, pressure and temperature surveys. The results of the previous simulation studies (Nakamura, 1986, and Sato, 1992) were also taken into account.

The model was then processed through history matching simulation to reproduce the pressures and temperatures at the wells. In simulation, total 48 wells (24 producers, and 24 injectors) were imposed on the model. Among 75 wells existing in the field, 27 wells could be either excluded because of negligible rates or combined with a nearby well in the same simulation cell. The recurrent data of the wells for about 13 years (4790 days) were applied to the model. The field total production and injection rates are shown in Fig. 2. The difference between production and injection, about 10,000 ton/day, is the steam flow utilized for power generation.

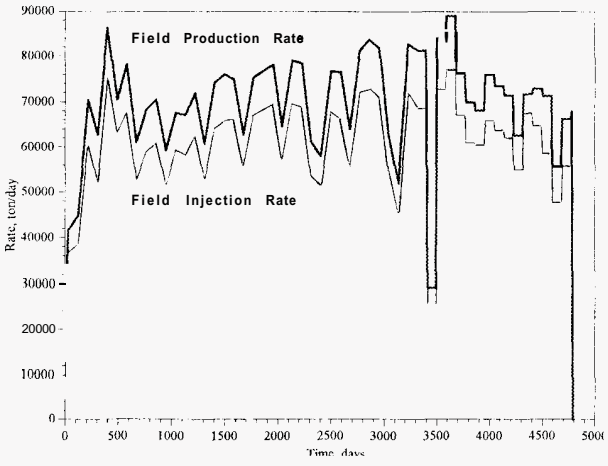

Fig. 2 - Field total production and injection rates.

2.1 Model Initialization

The field is gridded into 14 x 19 x 9 cells based on the reservoir geometry, the well locations and the completion zones. The plan view of gridding is shown in Fig. 3. As illustrated, the cells are made finer over the production and injection areas, and larger for surrounding area. Pore volumes of the aquifer cells are later determined by sensitivity runs where effects of changing the pore volumes of the outermost cells as well as the Layer 9 cells on pressure behaviours are studied. Large pore volumes are required for these cells as descibed later, which suggests the existence of the strong drive from the aquifer. Simulation layering is made as shown in Fig. 4. Upper-K and Middle-K formations are divided into two layers each to better model the main producing zones. Four structural

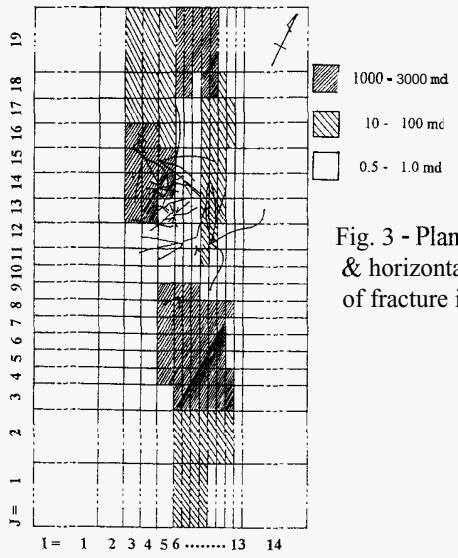

Fig. 3 - Planview gridding & horizontal permeability of fracture in Layer 5

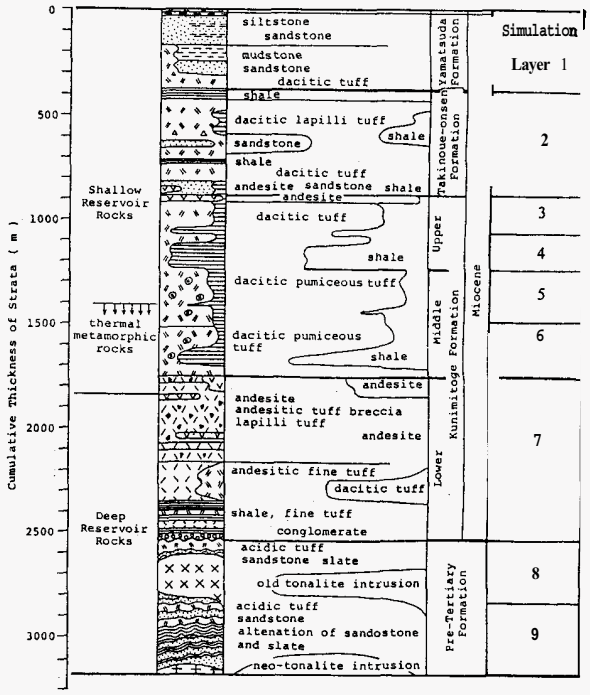

Fig. 4 - Schematic geologic sequence (after Kato et al., 1993) and simulation layering.

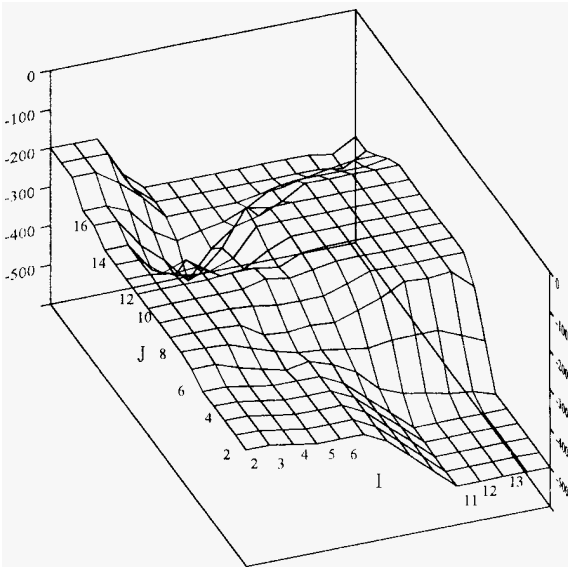

Fig. 5 - Structural top surface of Layer 5

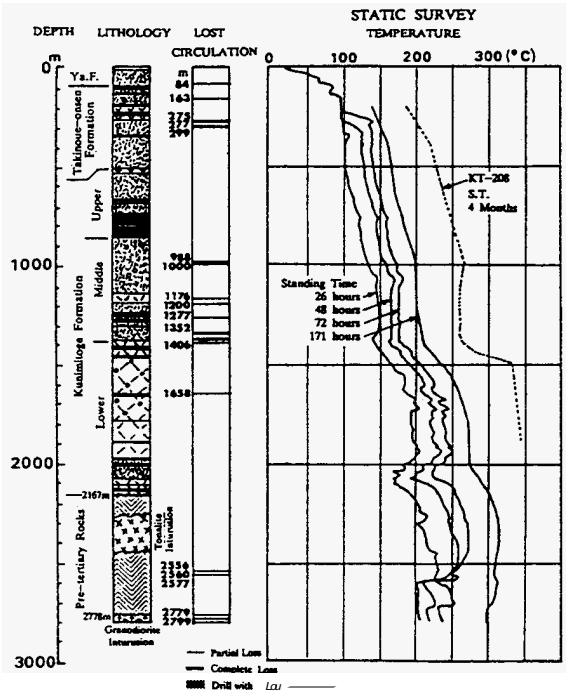

Fig. 6 - Geologic column and temperature surveys at the first deep production well K6-2. KT-208 is the exploration well (after Hanano & Takanohashi, 1993).

contour maps of the top surfaces of T formation, Upper-K, Middle-K and Lower-K formations are digitized and used as shape controls in constructing the model geometry. Fig. 5 is the top surface of Layer 5 of the simulation grids. This surface ranges from 200 m to 500 m subsea, has the highest point at the northwest end and the lowest at the southeast end, and shows a local depression at the northwest comer.

The horizontal locations of the production wells are concentrated in the grid region within I = 3 and 8, and J = 13 and 17, while the injection wells are located in two regions: the same area of the production wells, and the south part of the field within I = 5 and 12, and J = 6 and 7.

Based on the feed point data, completion layers are assigned to each production and injection well. Most production well are completed in Layers 5 and 6. A few wells are completed in each of Layers 3, 4 and 7, and one well in Layer 8. The injection wells drilled in the production area are completed in Layers 2 and 3, while the injectors in the south part are completed mainly in Layer 5.

The dual porosity option of the simulator is employed to properly simulate the observed pressure and temperature behaviours such that injected water quickly breaks through to nearby production wells, and that temperatures lowered by injected water also quickly recover when injection is stopped. Permeability and porosity are assigned to both matrix and fracture of the dual porosity model. A constant permeability 1 md is assigned for matrix rock in the horizontal and vertical directions. Matrix porosity is 18 % for Layer 1 and continuously decreased to 8 % for Layer 8. Fixed values 30 m and 0.5 % are used for fracture spacing and fracture porosity, respectively. As fracture spacing is fixed, actual heterogeneous distributions of the fracture density are taken into account by adjusting fracture permeability. Fracture development is dominant in Layer 5, and Layers 3 and 4 are also highly fractured.

The initial pressure distribution is calculated by assuming a constant pressure gradient 7.80 kPa/m over the whole depth (Hanano and Takanohashi, 1993), while the density of water is set so that the hydrostatic pressure is balanced to the pressure gradient. Temperatures of the initial model are set by using the temperature contour maps in nine horizons which were prepared by using the temperature surveys in the wells as shown in Fig. 6 (Hanano and Takanohashi, 1993).

2.2 History Matching

The history matching simulations are performed repeatedly until reasonable matchings are obtained for the pressure data at 24 wells and the temperature data at 20 wells. The aquifer size and fracture penneabilities are main parameters to be adjusted through the history matching process.

The extension of both the peripheral and bottom aquifers needs to be large enough to sustain average pressure levels. The outermost cells are modified to 3000 m in both horizontal directions. The cells in the row J = 2 are also enlarged to 1000 m in J direction. The pore volume of the bottom layer, Layer 9, is also adjusted to simulate a large volume of formation. This is done by increasing matrix porosity to 50 %.

Fracture permeability is locally adjusted to reproduce the pressure and temperature histories. Although both fracture porosity and fracture spacing vary spatially in reality, the fixed values are assigned to these parameters over the field. Thus the fracture permeabilities need to be adjusted to

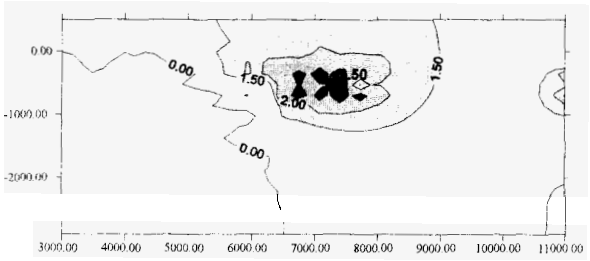

Fig. 7 - Horizontal permeability (md) of fracture in the cross-section, I = 4. Contours are log (k).

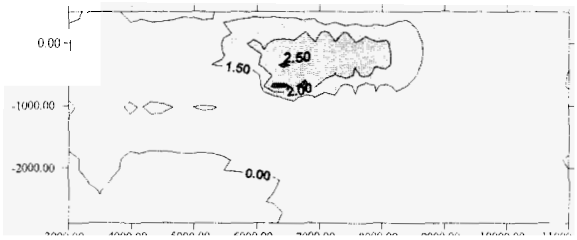

Fig. 8 - Vertical permeability (md) of fracture in the cross-section, I = 4. Contours are log(k).

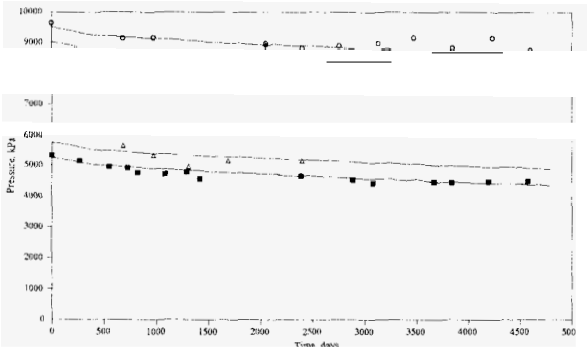

Fig. 9 - Typical history matching results of well pressures (not converted to datum).

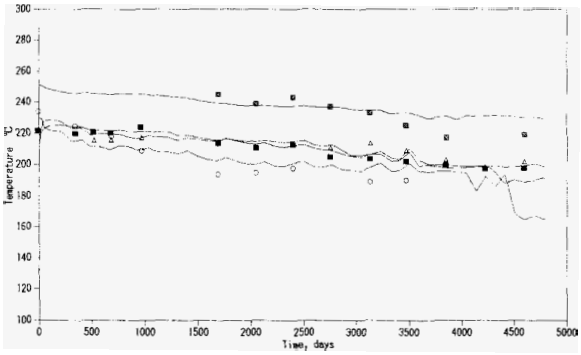

Fig. 10 - Typical history matching results of well temperatures.

account for compound effects of distributions of permeability, porosity, fracture density and others on water flow.

Fracture permeability is assumed to be laterally isotropic in each layer. Vertical permeability is generally lower than horizontal permeability, although history matching required vertical permeability locally as high as horizontal permeability. The general trends of the fracture permeability distribution in each layer are such that a highly fractured strip zone extends in northwest to southeast direction, and that the west and east sides of the field are tight. Layers 1, 2 and 7 are fractured to some extent, but to much less a degree than Layers 3 through 6. Layers 8 and 9 essentially are un-fractured. Horizontal permeabilities of fracture in Layer 5 are shown in Fig. 3. Figs. 7 and 8 show also the horizontal and vertical permeability distributions, respectively, in the cross-section, I = 4. Heterogeneous natures of the fracture development are seen in both figures. Fractures of permeability 1000 - 3000 md are developed only in the limited regions.

Some of the results of pressure matching are shown in Fig 9, where the pressure decline almost leveled off after about 10 years. Behavior of reservoir temperature is directly influenced by injected water, and therefore more complex as shown in Fig. 10.

In Fig. 11, the reservoir pressure distributions are shown as isobaric maps for Layer 4. At the end of history matching, 13.1 years, a high pressure slope has been

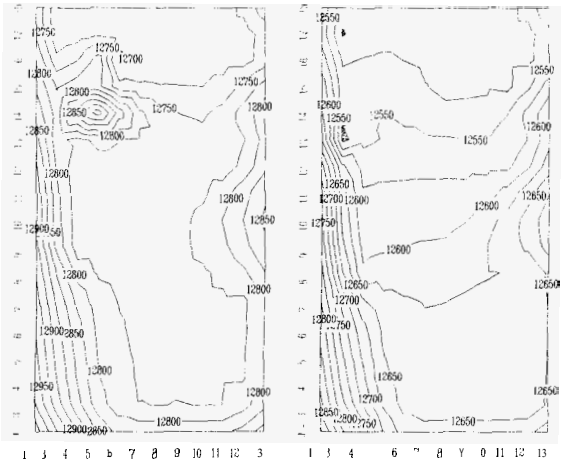

(a) **At** 3050 days (8 4 yrs) (b) **At** 4790 days (13 1 yrs)

Fig. 11 - Isobaric maps in Layer 4, in kPa at datum depth 1000 m subsea.

developed at the west side, and the pressure gently increases to south.

3. HYDROTHERMAL MECHANISMS

The Kakkonda geothermal field presents a unique feature such that a new reservoir was found over 1000 m deeper than the reservoir which had been produced for about 10 years. Multiple reservoirs at different depths are often seen in oil and gas fields, but unlike hydrocarbon reservoirs, the shallow and deeper reservoirs hydraulically

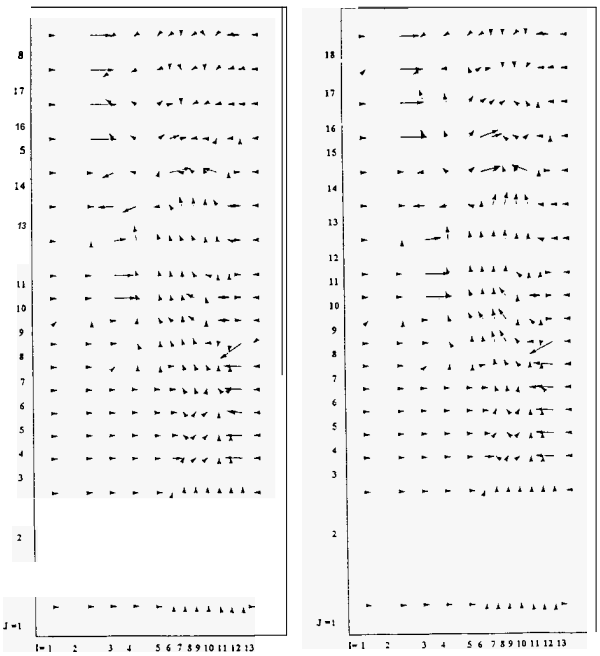

(a) **At** *3050* days (8.4 yrs). (b) **At** 4790 days (13.1 yrs).

Fig. 12 - Velosity fields in Layer 4.

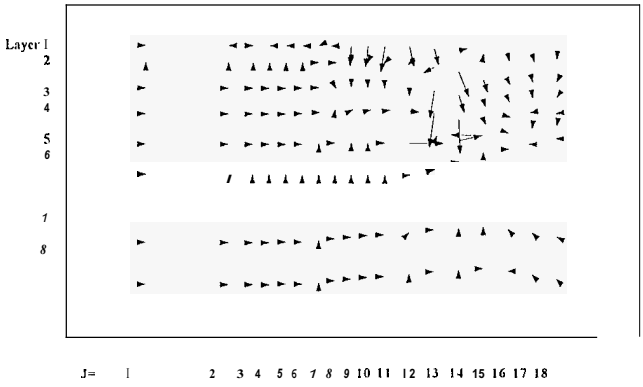

(a) **At** *3050* days (8.4 yrs)

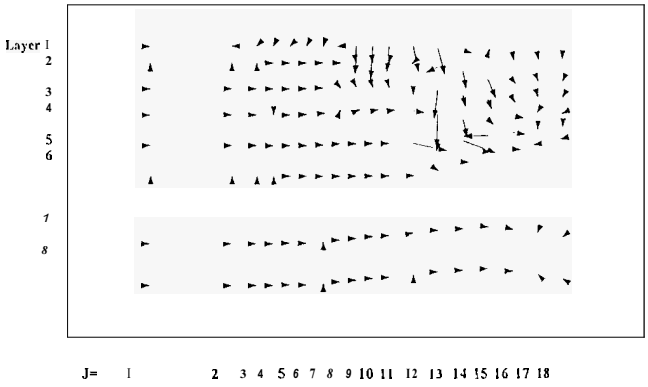

(b) **At** 4790 days (13 1 yrs)

Fig. 13 - Velosity fields in the cross-section, I = 4.

communicate each other. Understanding of hydrothermal mechnisms is highly necessary for successful development of the field.

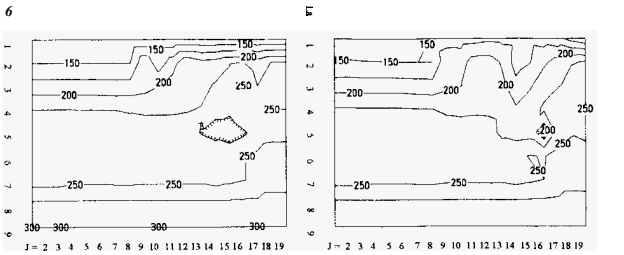

(a) **At** 0 days. (b) **At** *2050* days *(5.6* yrs).

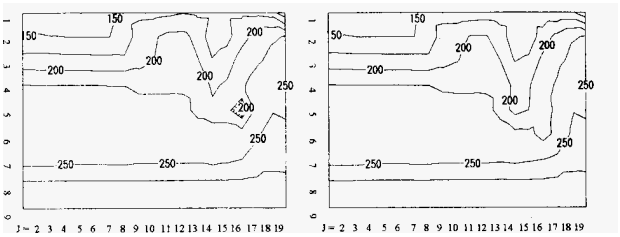

(c) **At** *3050* days (8.4 yrs). (d) **At** 4790 days(13.1 yrs).

Fig. 14 - Temperature transitions in the cross-section, I = 4.

As all the produced water is injected back into the shallow reservoir, hydrothermal mechanisms have been established in two ways: 1) heat extraction by water produced through natural fracture networks, and 2) continuous cooling flows created by injected water of about 150°C. These flow systems are extensively overlaid by influxes from the peripheral aquifer.

Fig. 12 shows a fluid velocity field in Layer 4, where lateral influxes are dominant over the field. **A** general trend of upward flow is also seen in the longitudinal direction in the lower half of the field. These significant water supplies from the surroundings are major resources to sustain the reservoir pressure. In the production area, clearly seen are several local flows, one of which is a strong radial flow at I = 5 and J = 15 in Fig. 12(b). This flow is created by water injected into Layer 2, two layers above.

Velocity fields in cross-section along I = 4 are shown in Fig. 13. **A** well aligned flow is dominant below Layer 3 in the left (south) half of the field. Within the production zone, however, strong cross-flows are noted. Water injection into Layer 2 in the production area is so influential that a spreading flow is induced in the lower layers. As seen in Fig. 13 (a), an upward flow in the tight formation, Layer **7** through 9, below the production zone is also important for sustaining the reservoir pressure.

Fig. 14 illustrates the temperature transitions in the cross-section also along I = 4, drawn from the simulation results. The temperature contours in the left (south) half are stable through the history. 250°C and higher temperatures in the lower part of the field also remain unchanged. Only remarkable a change is constant expansion of the 200°C contour in the production zone.

CONCLUSIONS

A numerical model was constructed for simulation studies of the Kakkonda geothermal field where the deeper reservoir had been discovered below the fully developed shallow reservoir. Several hydrothermal mechanisms were confirmed by the history matching of about 13 years field data. Fracture development in the upper reservoir is limited and highly heterogeneous. Through this fracture network, production and injection create strong active crossflows. With injection of about 85 % of extracted water, the reservoir pressure declined fust and then reached a stabilized level. Simulation showed horizontal influxes from the peripheral aquifer are most effective to sustain the reservoir pressure. Also confirmed by simulation is that the stabilized pressure of the shallow reservoir is partially supported by the lower tight formation. Simulation clearly demonstrated the temperature transitions within the productive zone such that the matrix rock region of 20 - 25°C lower than the original temperature is continuously expanding.

ACKNOWLEDGEMENTS

The authors would like to thank Japan Metals and Chemicals Co., Ltd. (JMC) and JMC Geothermal Engineering Co., Ltd. (JMC GeoE) for permission to publish this paper. The highest credit is to be given to the geoscientists and engineers of both JMC and JMC GeoE for their work of high quality.
The simulation model used is STARS developed by Computer Modelling Group in Calgary, Canada.

REFERENCES

Doi, N., Muramatsu, Y., Chiba, Y. and Tateno, M. (1988). *Geological Analysis of the Kakkonda Geothermal Reservoir.* Proceedings of International Symposium on Geothermal Energy, Kumamoto and Beppu, Japan, pp. 522-525.

Hanano, M. and Takanohashi, M. (1993). *Review of Recent Development of the Kakkonda Deep Reservoir, Japan.* Proceedings of the 18th Workshop on Geothermal Reservoir Engineering, Stanford University

Kasai, K., Kotanaka, K. and Chiba, F. (1990). Operation and Reservoir Management of the Kakkonda Geothermal Power Station. *Chinetsu (Jnl. of Japan Geothermal Energy Association),* Vol. 27, pp. 1-22. (In Japanese with English abstract)

Kato, O. and Doi, N. (1993). *Neo-Granitic Pluton and Later Hydrothermal Alteration at the Kakkonda Geothermal Fiels, Japan.* Proceedings of the 15th New Zealand Geothermal Workshop, pp. 155-161.

Kato, O., Doi, N. and Muramatsu, Y. (1993). Neo-Granitic Pluton and Geothermal Reservoir at the Kakkonda Geothermal Field, Iwate Prefecture, Japan. *Jnl. of Geothermal Research Society of Japan,* Vol. 15, No. 1, pp. 41-57. (In Japanese with English abstract)

Nakamura, H. (1986). *Flow of Hot Water in Geothermal Reservoir, Kakkonda, North-east Japan.* Proceedings of International Symposium "Geothermal Energy Development and Advanced Technology", Nov. 1986, Sendai, Japan, pp. 209-215. (In Japanese with English abstract)

Saito, S. (1993). The Drilling Experience of K6-2, the High-Temperature and Crooked Geothermal Well in Kakkonda, Japan. *Jnl. of Energy Resources Technology,* Vol. 115, No. 2, pp. 117-123.

Sato, K. (1982). Analysis of Geological Structure in the Takinoue Geothermal Area. *Jnl. of Geothermal Research Society of Japan*, Vol. 3, pp. 135-148.

Sato, K. (1992). *Management of Kakkonda Geothermal Power Plant.* Management Forum on Geothermal Development & Utilization, New Energy Foundation, pp. 5(2)-1 - 5(2)-26. (In Japanese)

Tosha, T., Sugihara, M. and Nishi, Y. (1993). *Microearthquake Activity at the Kakkonda Geothermal Field in ,Japan.* Proceedings of the 15th New Zealand Geothermal Workshop, pp. 175-179.